Journal of Magnetic Resonance 200 (2009) 261–266

Contents lists available at ScienceDirect

Journal of Magnetic Resonance

journal homepage: www.elsevier.com/locate/jmr

Study of nuclear quadrupole interactions and quadrupole Raman processes of ^{69}Ga and ^{71}Ga in a β-Ga_2O_3:Cr^{3+} single crystal

Tae Ho Yeom [a], Ae Ran Lim [b,*]

[a] Division of Applied Science, Cheongju University, Cheongju 360-764, Republic of Korea
[b] Department of Science Education, Jeonju University, Jeonju 560-759, Republic of Korea

ARTICLE INFO

Article history:
Received 15 April 2009
Revised 14 June 2009
Available online 6 August 2009

Keywords:
Nuclear magnetic resonance
Crystal growth
Optical materials
Relaxation times

ABSTRACT

Nuclear magnetic resonance (NMR) data and the spin–lattice relaxation times, T_1, of ^{69}Ga and ^{71}Ga nuclei in a β-Ga_2O_3:Cr^{3+} single crystal were obtained using FT NMR spectrometry. Four sets of NMR spectra for ^{69}Ga ($I = 3/2$) and ^{71}Ga ($I = 3/2$) were obtained in the crystallographic planes. The ^{69}Ga and ^{71}Ga nuclei each had two chemically inequivalent Ga_I and Ga_{II} centers. Each of the ^{69}Ga and ^{71}Ga isotopes yielded two different central NMR resonance lines originating from Ga_I and Ga_{II} sites. The nuclear quadrupole coupling constants and asymmetry parameters of $^{69}Ga_I$, $^{69}Ga_{II}$, $^{71}Ga_I$, and $^{71}Ga_{II}$ centers in a β-Ga_2O_3:Cr^{3+} crystal were obtained. Analysis of the EFG tensor principal axes (PAs) for Ga nuclei and the ZFS tensor PAs for the Cr^{3+} ion confirmed that the Cr^{3+} paramagnetic impurity ion substitutes for the Ga^{3+} ion in the oxygen octahedron. In addition, the temperature dependencies of the ^{69}Ga and ^{71}Ga relaxation rates were consistent with Raman processes, as $T_1^{-1} \propto T^2$. Even though the Cr^{3+} impurities are paramagnetic, the relaxations were dominated by electric quadrupole interactions of the nuclear spins in the temperature range investigated.

1. Introduction

Transparent conducting oxides (TCOs) are key materials in state-of-the-art optoelectronics. TCOs are used in a variety of devices including flat-panel displays and solar energy conversion devices. Among the TCOs reported to date, gallium oxide (β-Ga_2O_3) has the widest band gap energy of 4.8 eV [1], is transparent from the visible into the UV region [2], and demonstrates thermal stability because of a high melting point [3]. Interest in β-Ga_2O_3 continues, because it is a relatively new material with a number of potential applications in optoelectronics and gas sensing. β-Ga_2O_3 may also be used as a host material in electroluminescent devices [4,5]. β-Ga_2O_3 is intrinsically an insulator with a band gap of 4.8 eV. The material becomes n-type semiconducting when synthesized under reducing conditions. The n-type semiconductivity is known to arise because of a slight oxygen deficit in the crystal lattice [6]. The electrical conductivity of β-Ga_2O_3 at elevated temperatures is markedly and reversibly altered in the presence of oxidizing or reducing gases.

β-Ga_2O_3 has a monoclinic crystal structure and belongs to the space group C_{2h}^3–$C2/m$ with lattice parameters $a = 1.2214$ nm, $b = 0.30371$ nm, and $c = 0.57981$ nm, and $\beta = 103.83°$ [7–9]. Melting points of $T_m = 1740$ °C [7,8] or 1807 °C [10] have been reported in the literature. The unit cell contains four Ga_2O_3 molecules. Two chemically distinguishable cationic sites are coordinated either tetrahedrally or octahedrally with oxygen ions. The crystal structure is a double chain of GaO_6 octahedra, Ga_I, arranged parallel to the *b*-axis of the lattice, which is connected by GaO_4 tetrahedra, Ga_{II}, as shown in Fig. 1. The crystal has two cleavage planes, perpendicular to the *a*- and *c*-axes, respectively.

A nuclear magnetic resonance (NMR) study of ^{69}Ga and ^{71}Ga nuclei in pure β-Ga_2O_3 single crystals grown by the Verneuil method [11] has been performed [12]. These studies, which disclosed all ^{69}Ga and ^{71}Ga resonances, yielded eight sets of NMR parameters; these eight sets of resonance lines originated from a twin structure. Also, electron paramagnetic resonance (EPR) studies of Cr^{3+} [13,14] in β-Ga_2O_3 single crystals have been reported.

The spin–lattice relaxation times of nuclei in a crystal reflect crystal dynamics, such as nucleus–phonon interactions, and indicate how easily the excited state energy of the nuclear system can be transferred into the lattice. In the present study, the behavior of Ga in a β-Ga_2O_3:Cr^{3+} single crystal was explored using NMR and relaxation time measurements. To obtain detailed information on crystal dynamics, it was necessary to measure spin–lattice relaxation times, T_1, of constituent ^{69}Ga and ^{71}Ga nuclei.

In the present study, the NMR properties of ^{69}Ga and ^{71}Ga in a β-Ga_2O_3:Cr^{3+} single crystal were investigated using a Pulse NMR spectrometer. Four sets of Ga NMR spectra were obtained in the crystallographic planes at room temperature and analyzed using

* Corresponding author. Fax: +82 (0)63 220 2053.
E-mail addresses: aeranlim@hanmail.net, arlim@jj.ac.kr (A.R. Lim).

1090-7807/$ - see front matter © 2009 Elsevier Inc. All rights reserved.
doi:10.1016/j.jmr.2009.07.008

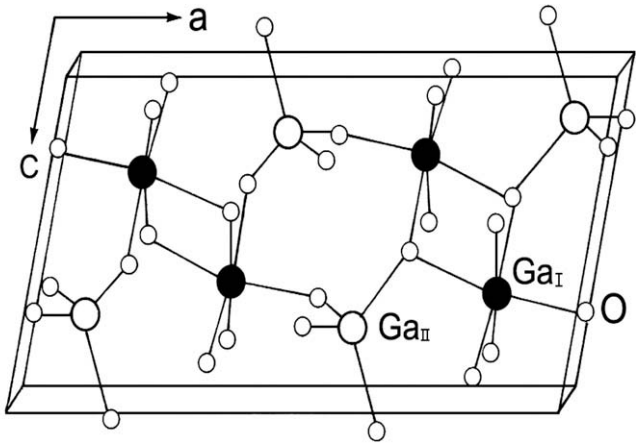

Fig. 1. Projection of the β-Ga_2O_3 single crystal unit cell structure onto the *ca*-plane.

the Zeman and nuclear quadrupole Hamiltonians. The quadrupole coupling constants (e^2qQ/h), asymmetry parameters (η), and directions of the principal tensor axes of electric field gradients (EFGs) of the ^{69}Ga and ^{71}Ga centers in the β-Ga_2O_3:Cr^{3+} single crystal were determined and compared with those of previous reports. In addition, the spin–lattice relaxation times, T_1, of both ^{69}Ga and ^{71}Ga nuclei were investigated in detail as a function of temperature. This work will enhance understanding of nuclear relaxation processes in the crystal.

2. Experimental

Single crystals of β-Ga_2O_3 doped with Cr^{3+} (0.05 mol%) were grown using a floating zone method [14]. Crystallographic axes were determined by the X-ray Laue approach. No twin domain structure was found by X-ray, NMR, or EPR. Ga NMR measurements were conducted using a Bruker FT NMR spectrometer (MSL 200 model) of the Korea Basic Science Institute. The static magnetic field was 4.7 T and central rf frequencies for ^{69}Ga and ^{71}Ga nuclei were set at $\omega_0/2\pi = 48.0372$ MHz and $\omega_0/2\pi = 61.0296$ MHz, respectively. The free induction decay (FID) of ^{69}Ga and ^{71}Ga NMR was recorded with a single pulse sequence, 5000 scans, and a repetition time of 0.5 s on each crystallographic plane. A pulse length of 1 μs (90° pulse) was used. For T_1 measurements, a π–t–$\pi/2$ inversion recovery pulse sequence was employed. The width of the π pulse was 2 μs for both ^{69}Ga and ^{71}Ga. Sample temperatures were maintained at constant values by controlling helium flow and heater current, with an accuracy of ±0.5 °C.

Typical NMR spectra of ^{69}Ga and ^{71}Ga in the β-Ga_2O_3:Cr^{3+} crystal in an arbitrary external magnetic field at room temperature are shown in Fig. 2(a) and (b), respectively. These spectra were obtained by Fourier transforming the FID of Ga ($I = 3/2$) NMR. Only central resonance lines are observed because of a large quadrupole interaction. The spectra of each of the ^{69}Ga and ^{71}Ga nuclei consist of two sets of resonance lines, denoted as Ga_I at the six-oxygen octahedron (Ga_I center) and Ga_{II} at the four-oxygen tetrahedron (Ga_{II} center). The resonance lines from ^{69}Ga at the octahedral site and ^{69}Ga at the tetrahedral site are designated the $^{69}Ga_I$ center and the $^{69}Ga_{II}$ center, respectively. The resonance lines from ^{71}Ga at the octahedral site and ^{71}Ga at the tetrahedral site are termed the $^{71}Ga_I$ center and the $^{71}Ga_{II}$ center, respectively. The central line widths of the $^{69}Ga_I$, $^{69}Ga_{II}$, $^{71}Ga_I$, and $^{71}Ga_{II}$ centers were $(\Delta\nu)_{FWHM} \approx 5.0$–$5.8$ kHz, depending on the direction of the applied field with respect to the crystallographic axes.

We defined five directions as follows: *a*, *b*, *c*, *a**, and *c**. The first three directions are those of the principal crystallographic axes, and the last two are perpendicular to the *bc*-plane and *ab*-plane,

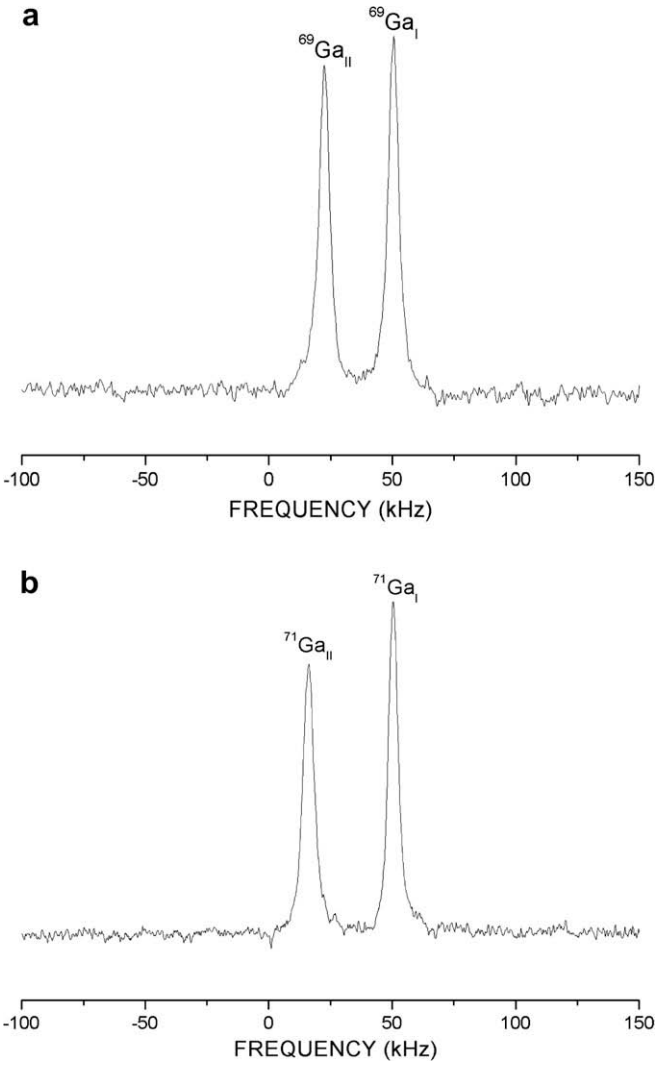

Fig. 2. Typical NMR absorption spectra of (a) ^{69}Ga and (b) ^{71}Ga nuclei in a β-Ga_2O_3:Cr^{3+} single crystal at room temperature.

respectively. The resonance absorption spectra of ^{69}Ga and ^{71}Ga nuclei in the β-Ga_2O_3:Cr^{3+} crystal were observed at intervals of 10° as the crystal was rotated through 180°. The experimental resonance frequencies of ^{69}Ga and ^{71}Ga nuclei measured on the crystallographic *ba***b*- and *bc***b*-planes are plotted in Figs. 3 and 4 as closed circles and closed rectangles, respectively, together with other data calculated as described below.

The resonance frequencies changed during crystal rotation with respect to the magnetic field. To obtain the actual Ga NMR frequencies in Figs. 3 and 4, 48.0372 MHz and 61.0294 MHz should be added to the frequencies in the graphs for ^{69}Ga and ^{71}Ga, respectively. The rotational angles in Figs. 3 and 4 are with reference to the crystallographic *b*-axis. We tried to adjust crystal mounting so that NMR spectral extrema along the *b*-axis in the *ba***b*- and *bc***b*-planes coincided. The crystallographic data show that the *b*-axis is parallel to the monoclinic direction of the crystal, consistent with previous reports [3,9].

3. Analysis and discussion

3.1. e^2qQ/h and η of ^{69}Ga and ^{71}Ga nuclei

NMR spectra of ^{69}Ga ($I = 3/2$, natural abundance 60.4%) and ^{71}Ga ($I = 3/2$, natural abundance 39.6%) centers were analyzed with the

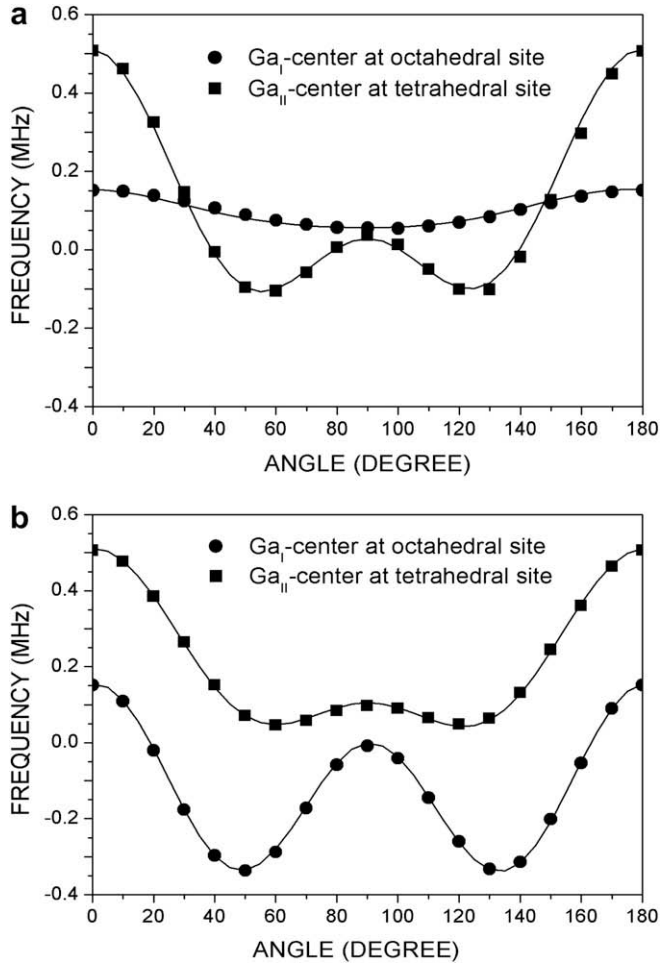

Fig. 3. Rotation patterns of nuclear magnetic resonance frequencies for the ^{69}Ga nucleus in (a) the ba^*b-plane and (b) the bc^*b-plane. The experimental data at octahedral and tetrahedral sites of ^{69}Ga centers are plotted using solid circles and solid rectangles, respectively. The solid lines are calculated resonance frequencies obtained from simulations using the parameters in Table 1.

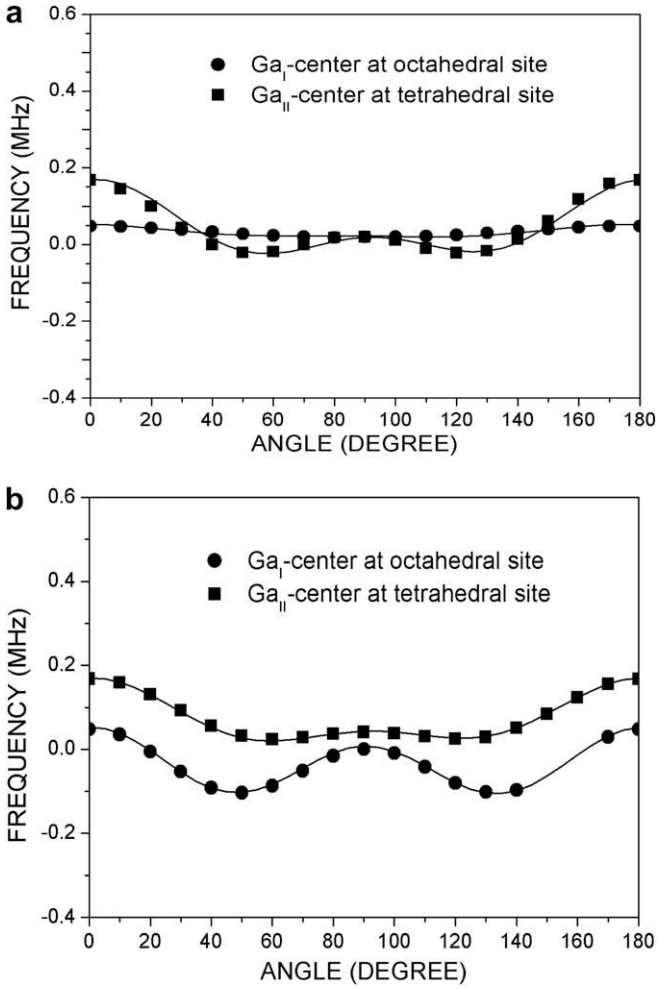

Fig. 4. Rotation patterns of nuclear magnetic resonance frequencies for the ^{71}Ga nucleus in (a) the ba^*b-plane and (b) the bc^*b-plane. The experimental data from octahedral and tetrahedral sites with ^{71}Ga centers are plotted using solid circles and solid rectangles, respectively. The solid lines are calculated resonance frequencies obtained from simulations using the parameters in Table 1.

usual Hamiltonian. The e^2qQ/h and η values, and the EFG tensor directions for the ^{69}Ga and ^{71}Ga nuclei in the β-Ga_2O_3 crystal were determined using a computer program (EPR/NMR version 6.0) [15] with exact diagonalization of the Hamiltonian matrices. Here the "laboratory" axes used for Hamiltonian analysis are labeled with lowercase letters (x, y, z). These were chosen to coincide with the crystallographic axes a, b, and c^*. The principal EFG tensor axes are labeled with uppercase letters (X, Y, Z). The input parameter set was optimized using a nonlinear least-squares routine, to minimize weighted differences between observed and calculated transition frequencies.

NMR absorption spectra of Ga nuclei in a β-Ga_2O_3:Cr^{3+} single crystal were observed in the crystallographic ba^*b- and bc^*b-planes. There are four molecules of Ga_2O_3 in the unit cell. There are two chemically nonequivalent gallium ion groups. One group is at the octahedral site Ga_I and the other at the tetrahedral site Ga_{II}. The four Ga nuclei of Ga_I site in the unit cell were magnetically and chemically equivalent, as were the other four Ga nuclei of Ga_{II}. Therefore, only two distinct sets of resonance lines can be obtained by Ga NMR of the unit cell: one set from the Ga_I center and the other from the Ga_{II} center. In our experiments, however, four different central resonance lines of Ga nuclei were obtained on each crystallographic plane, as shown in Figs. 3 and 4. It transpired that the Ga nuclei (Ga_I center) at the oxygen octahedron yielded two different central resonance lines because the Ga atoms were a mixture of the isotopes ^{69}Ga and ^{71}Ga, as did nuclei at the Ga_{II} center. Thus, four NMR absorption spectra from $^{69}Ga_I$, $^{69}Ga_{II}$, $^{71}Ga_I$, and $^{71}Ga_{II}$ centers were observed in each of the crystallographic ba^*b- and bc^*b-planes.

The final best fits of the e^2qQ/h and η values for Ga nuclei are listed in Table 1. The nuclear quadrupole coupling constants of $^{69}Ga_I$, $^{69}Ga_{II}$, $^{71}Ga_I$, and $^{71}Ga_{II}$ centers in the β-Ga_2O_3:Cr^{3+} single crystal were 13.11 MHz, 17.74 MHz, 8.24 MHz, and 11.16 MHz at room temperature, respectively. The asymmetry parameters (η) of the $^{69}Ga_I$, $^{69}Ga_{II}$, $^{71}Ga_I$, and $^{71}Ga_{II}$ centers were 0.15, 0.86, 0.14, and 0.87 at room temperature, respectively. Simulations of resonance fields for $^{69}Ga_I$, $^{69}Ga_{II}$, $^{71}Ga_I$, and $^{71}Ga_{II}$ centers were performed using the parameters in Table 1, and simulations of rotation patterns in the ba^*b- and bc^*b-planes are shown in Figs. 3 and 4 as solid lines. The lines fit the experimental data well.

Table 1
Nuclear quadrupole coupling constants, e^2qQ/h, and asymmetry parameters, η, of Ga centers in β-Ga_2O_3 single crystal.

Nucleus	e^2qQ/h (MHz)	η
$^{69}Ga_I$	13.11 ± 0.15	0.15 ± 0.01
$^{69}Ga_{II}$	17.74 ± 0.15	0.86 ± 0.01
$^{71}Ga_I$	8.24 ± 0.10	0.14 ± 0.01
$^{71}Ga_{II}$	11.16 ± 0.10	0.87 ± 0.01

The nuclear quadrupole coupling constants of $^{69}Ga_I$ (13.11 MHz) and $^{69}Ga_{II}$ (17.74 MHz) were larger than those of $^{71}Ga_I$ (8.24 MHz) and $^{71}Ga_{II}$ (11.16 MHz), because the electric quadrupole moment of ^{69}Ga nuclei (0.168×10^{-24} cm^2) is larger than that of ^{71}Ga nuclei (0.106×10^{-24} cm^2). The nuclear quadrupole coupling constant ratios of $e^2qQ/h(^{69}Ga_I)/e^2qQ/h(^{71}Ga_I)$ at the octahedral site and $e^2qQ/h(^{69}Ga_{II})/e^2qQ/h(^{71}Ga_{II})$ at the tetrahedral site were both 1.59. The asymmetry parameters of $^{69}Ga_I$ (0.15) and $^{71}Ga_I$ (0.14) at octahedral sites were the same, within experimental accuracy, because the ^{69}Ga and ^{71}Ga isotopes reside in identical octahedral environments and have the same EFGs. Similar results were obtained for $^{69}Ga_{II}$ (0.86) and $^{71}Ga_{II}$ (0.87) at tetrahedral sites.

The zero-field splitting (ZFS) parameter D of a paramagnetic ion is proportional to the nuclear quadrupole coupling constant e^2qQ/h [16]. ZFS parameters seem to be related to the crystal field (CF) parameters. The ZFS parameter D may be proportional to e^2qQ/h if there is some relationship between CF and ZFS. There is also formal similarity, but no physical similarity, between D and e^2qQ/h in the EPR and NMR Hamiltonians. The EFG values at Ga sites can be calculated using e^2qQ/h values from NMR. The principal axes (PAs) of D tensors may be proportional to PAs of EFG tensors. The PAs of the EFG tensors for $^{69}Ga_I$, $^{69}Ga_{II}$, $^{71}Ga_I$, and $^{71}Ga_{II}$ centers in the β-Ga_2O_3 single crystal are listed in Table 2. If the right-handed axis system of Ref. [14] is used, the PAs of the D tensors for Cr^{3+} in the β-Ga_2O_3:Cr^{3+} single crystal in Ref. [14] are similar to the PAs of the EFG tensors (Table 2) for $^{69}Ga_I$ and $^{71}Ga_I$ centers at the octahedral site rather than the tetrahedral site. This means that Cr^{3+} ions in β-Ga_2O_3:Cr^{3+} replace the Ga_I^{3+} ions in oxygen octahedral but not Ga_{II}^{3+} ions in the oxygen tetrahedral. According to the previous report [14], Cr^{3+} ions replace Ga_I^{3+} ions in oxygen octahedral from the EPR study of Cr^{3+} in a β-Ga_2O_3. Therefore, our NMR results confirm that Cr^{3+} ions replace the Ga_I^{3+} ions in the oxygen octahedra.

Vosegaard and colleagues [12] reported ^{69}Ga and ^{71}Ga NMR data from pure β-Ga_2O_3 single crystals grown by the Verneuil method. These authors observed all ^{69}Ga and ^{71}Ga resonances and presented eight sets of NMR parameters in Table 1 of Ref. [12]. The eight sets of resonance lines are consistent with a twin structure because twinning characteristics leading to multiple lines in EPR and NMR spectra can be observed in their data. However, the β-Ga_2O_3:Cr^{3+} single crystal used in our study did not have a twin structure, as confirmed by preliminary X-ray, NMR, and EPR experiments. Our NMR parameters for Ga nuclei in a crystal of β-Ga_2O_3 doped with Cr^{3+} were the same as those of Ga nuclei in the pure β-Ga_2O_3 crystal [12], within experimental accuracy, as can be seen in Table 1. The influence of Cr^{3+} (0.05 mol%) on Ga nuclei in the β-Ga_2O_3 crystal is thus negligible. Wolten and Chase [17] claimed that the crystal symmetry of the β-Ga_2O_3 crystal was triclinic (space group $P1$) rather than monoclinic. However, the crystal symmetry of β-Ga_2O_3 single crystals used in our experiments was monoclinic, and not triclinic, based on NMR and previous EPR [14] studies. This result is consistent with those of Geller [3] and Vosegaard and colleagues [12], who found monoclinic symmetry of the β-Ga_2O_3 crystal.

Table 2
The direction of EFG tensor of Ga centers in β-Ga_2O_3 single crystal. θ and φ are the angles from the reference rectangular axes, x, y, and z.

Nucleus		V_{XX}	V_{YY}	V_{ZZ}
$^{69}Ga_I$	θ (°)	94	89	4
	φ (°)	355	84	346
$^{69}Ga_{II}$	θ (°)	89	6	84
	φ (°)	90	185	359
$^{71}Ga_I$	θ (°)	97	89	3
	φ (°)	355	84	341
$^{71}Ga_{II}$	θ (°)	89	6	84
	φ (°)	91	190	1

3.2. Spin–lattice relaxation times of ^{69}Ga and ^{71}Ga nuclei

Usually, the effect of paramagnetic ions dominates the spin–phonon interaction for the relaxation time T_1 at very low temperature. Another major contribution to the spin–lattice relaxation for the nuclear spin $I \geqslant 1$ may be the quadrupolar interaction of the electric quadrupole moment of the nucleus with the lattice vibration. In the direct Raman process, the spin–lattice relaxation rate $1/T_1$ is proportional to the absolute temperature T [18]. On the other hand, the Raman process provides the relaxation rate proportional to the square of temperature in the high temperature limit [19–22].

We now describe recovery laws for quadrupole relaxation processes in ^{69}Ga ($I = 3/2$) and ^{71}Ga ($I = 3/2$) nuclear spin systems. The temperature dependence of the relaxation time is indicative of fluctuations in the EFG tensor driven by thermally activated motion. For $I = 3/2$, relaxation transition probabilities can be described by [20,23,24]:

$$W_1 = \frac{1}{12}\left[\frac{eQ}{\hbar}\right]^2 \int_{-\infty}^{\infty} \langle V_1(0)V_{-1}(t)\rangle \exp(i\omega_L t)dt$$

$$W_2 = \frac{1}{12}\left[\frac{eQ}{\hbar}\right]^2 \int_{-\infty}^{\infty} \langle V_2(0)V_{-2}(t)\rangle \exp(i2\omega_L t)dt \quad (1)$$

where W_1 and W_2 ($n = 1, 2$) are the ^{69}Ga and ^{71}Ga spin–lattice transition rates corresponding to the $\Delta m = \pm 1$ and $\Delta m = \pm 2$ transitions, respectively.

The inversion recovery traces for the central lines of ^{69}Ga and ^{71}Ga, respectively, with dominant quadrupole relaxation in Ga_2O_3, can be represented by the following combination of two exponential functions [25,26]:

$$[S(\infty) - S(t)]/2S(\infty) = 0.5[\exp(-2W_1 t) + \exp(-2W_2 t)] \quad (2)$$

Thus, the spin–lattice relaxation time is given by:

$$1/T_1 = \frac{2}{5}(W_1 + 4W_2) \quad (3)$$

The nuclear magnetization recovery traces for ^{69}Ga and ^{71}Ga were measured at several temperatures, and it was found that the inversion recovery traces could be represented by a combination of two exponential functions as in Eq. (2). The Ga_I and Ga_{II} resonance lines for ^{69}Ga and ^{71}Ga were displaced by a paramagnetic shift to higher frequency side relative to the reference signal ($\omega_0/2\pi = 48.0372$ MHz and $\omega_0/2\pi = 61.0296$ MHz for ^{69}Ga and ^{71}Ga nuclei, respectively) obtained for the ^{69}Ga resonance line from an aqueous solution of $Ga(NO_3)_3$. The isotropic chemical shift of the Ga_I and Ga_{II} is shifted by the Cr^{3+} doping.

The inversion recovery traces for the two central resonance lines of ^{69}Ga and ^{71}Ga nuclei in Ga_2O_3 crystals showing dominant quadrupole relaxation were measured, and one trace (that of ^{69}Ga), as a function of delay time at room temperature, is shown in Fig. 5. The inversion recovery traces differed depending on the measurement temperature. The $^{69}Ga_I$, $^{69}Ga_{II}$, $^{71}Ga_I$, and $^{71}Ga_{II}$ spin–lattice transition rates W_1 and W_2 were calculated using Eq. (3); W_1 was smaller than W_2, and W_1 and W_2 exhibited similar temperature dependencies. We measured variations in relaxation times with temperature for the four resonance lines of the $^{69}Ga_I$, $^{69}Ga_{II}$, $^{71}Ga_I$, and $^{71}Ga_{II}$ nuclei, respectively. The temperature dependencies of T_1 for $^{69}Ga_I$, $^{69}Ga_{II}$, $^{71}Ga_I$, and $^{71}Ga_{II}$ were obtained in terms of W_1 and W_2, and the results are shown in Fig. 6. The spin–lattice relaxation rates, T_1^{-1}, increased with increasing temperature. The T_1^{-1} values of ^{69}Ga and ^{71}Ga in the octahedral

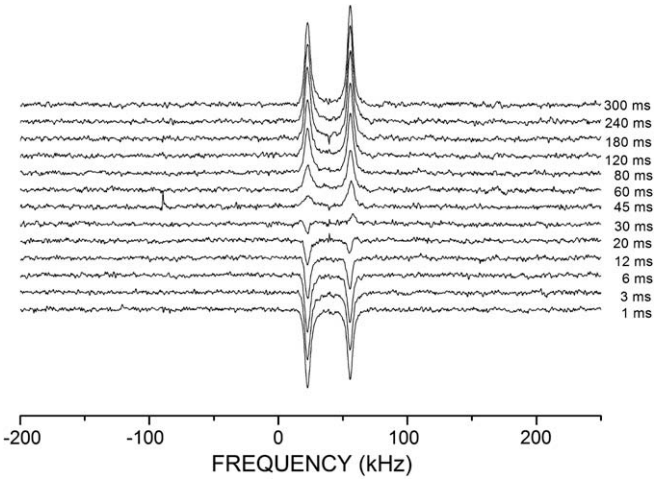

Fig. 5. Inversion recovery behavior of $^{69}Ga_I$ and $^{69}Ga_{II}$ at room temperature in β-Ga_2O_3:Cr^{3+} crystals as a function of delay time t.

environment (Ga_I) and in the tetrahedral environment (Ga_{II}) are very similar. Our experimental T_1 observations on ^{69}Ga and ^{71}Ga nuclei can be described using the equation $T_1^{-1} = AT^2 + B$; these calculations are shown as solid curves in Fig. 6.

Our data can be explained by the following relaxation mechanism: lattice vibrations are coupled to nuclear electric quadrupole moments by the dominant Raman processes (i.e., by absorption of one phonon ω and emission of another ω'). Here, the frequencies ω and ω' of the two phonons satisfy the energy conservation relation $\omega - \omega' = \omega_0$ (where ω_0 is the nuclear Larmor frequency), so that all phonons inside the phonon spectrum contribute to the relaxation processes. The Raman-induced spin–lattice relaxation rate is then independent of the Larmor frequency. From the Debye approximation for the phonon density of states [20]:

$$\left(\frac{1}{T_1}\right)_{\text{Raman}} = K\int_0^{\theta}\frac{\exp\{T'/T\}}{(\exp\{T'/T\}-1)^2}\left(\frac{T'}{\theta}\right)^6 dT' \quad (4)$$

where θ is the Debye temperature. For $T \geqslant \theta$, the temperature dependence is $T_1^{-1} \propto T^2$. The temperature dependencies of the spin–lattice relaxation rates, T_1^{-1}, of $^{69}Ga_I$, $^{69}Ga_{II}$, $^{71}Ga_I$, and $^{71}Ga_{II}$ are shown in Fig. 6. The rates are proportional to the square of temperature, T^k ($k = 2$), for the nuclei in the investigated temperature range (solid lines in Fig. 6). Therefore, the temperature dependencies of the ^{69}Ga and ^{71}Ga relaxation rates in Ga_2O_3:Cr^{3+} crystal are in accordance with Raman processes. The Raman process ($k = 2$) is more effective than the direct process ($k = 1$) for nuclear quadrupole relaxation in our experiments.

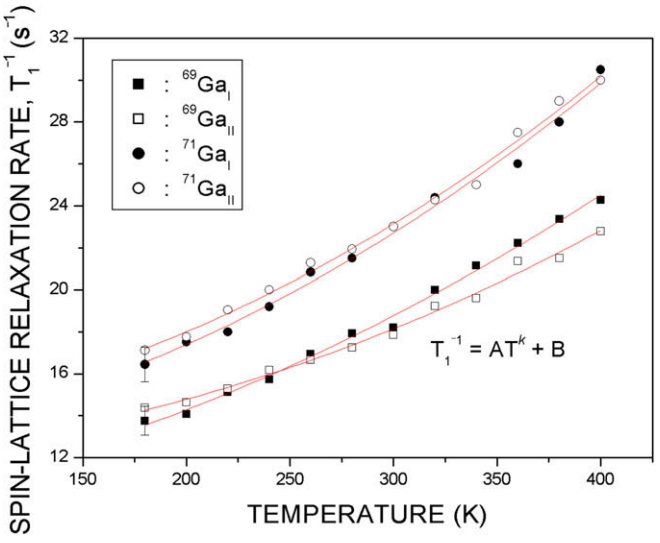

Fig. 6. Temperature dependencies of spin–lattice relaxation rates, T_1^{-1}, for ^{69}Ga and ^{71}Ga in β-Ga_2O_3:Cr^{3+} crystals. Solid curves represent fits obtained using the function $T_1^{-1} = AT^k + B$.

The relaxation rates for $^{71}Ga_I$ and $^{71}Ga_{II}$ nuclei are greater than those for $^{69}Ga_I$ and $^{69}Ga_{II}$ nuclei. The large difference of the spin–lattice relaxation time between ^{69}Ga and ^{71}Ga can be explained by the difference between their electric quadrupole moments. When the main relaxation mechanism of the Raman process due to the electric quadrupole interaction takes place, $1/T_1$ is a function of electric quadrupole moments [20,27].

Usually, the effect of paramagnetic ions dominates the spin–phonon interaction for the relaxation time T_1 at very low temperature. However, the paramagnetic Cr^{3+} impurity effect on the spin–lattice relaxation process of Ga nuclei in β-Ga_2O_3:Cr^{3+} crystal was found to be very weak in the experimental temperature range.

4. Conclusions

The nuclear quadrupole interaction constants, asymmetry parameters, and principal EFG tensor axes of the $^{69}Ga_I$, $^{69}Ga_{II}$, $^{71}Ga_I$, and $^{71}Ga_{II}$ nuclei in a β-Ga_2O_3:Cr^{3+} single crystal were obtained. The nuclear quadrupole interactions of the host nuclei in the crystal were investigated by determining NMR parameters and spin–lattice relaxation times. Four sets of resonance lines for Ga nuclei were observed in the crystallographic ba^*b- and bc^*b-planes. Considering crystal symmetry and Ga isotope distribution, the four sets of lines were found to originate from $^{69}Ga_I$ and $^{71}Ga_I$ centers at oxygen octahedra and $^{69}Ga_{II}$ and $^{71}Ga_{II}$ centers at oxygen tetrahedra. The e^2qQ/h and η values were 13.11 MHz and 0.15 for the $^{69}Ga_I$ center, 17.74 MHz and 0.86 for the $^{69}Ga_{II}$ center, 8.24 MHz and 0.14 for the $^{71}Ga_I$ center, and 11.16 MHz and 0.87 for the $^{71}Ga_{II}$ center. The principal X, Y, and Z EFG tensor axes for the four Ga centers were obtained. The e^2qQ/h and η values of the four Ga centers in a β-Ga_2O_3 single crystal doped with Cr^{3+} were the same as those of a pure β-Ga_2O_3 single crystal in Ref. [12], within the experimental accuracy; the only difference is that a twin structure was seen in Ref. [12] but not in the present work. We confirmed that Cr^{3+} impurity ions replace Ga_I^{3+} ions, by comparison of the EFG tensor axes for Ga nuclei and the ZFS tensor axes for the Cr^{3+} ion.

The relaxation mechanism was investigated by determining the spin–lattice relaxation times of the $^{69}Ga_I$, $^{69}Ga_{II}$, $^{71}Ga_I$, and $^{71}Ga_{II}$ nuclei in a β-Ga_2O_3:Cr^{3+} single crystal. The e^2qQ/h value for ^{69}Ga was larger than that for ^{71}Ga, in line with the finding that the T_1 of ^{69}Ga was longer than that of ^{71}Ga. The dominant relaxation mechanism for nuclei possessing electric quadrupole moments involves coupling of these moments to thermal fluctuations in the local EFGs via Raman spin–phonon processes. The relaxation rates of the ^{69}Ga and ^{71}Ga nuclei were found to increase with increasing temperature, and could be described using the equation $T_1^{-1} = AT^k + B$. The temperature dependence of the ^{69}Ga and ^{71}Ga relaxation rates in β-Ga_2O_3:Cr^{3+} crystals is in accordance with the well-known Raman process, as $T_1^{-1} \propto T^2$. The T_1 values for ^{69}Ga and ^{71}Ga in β-Ga_2O_3:Cr^{3+} crystals can be explained in terms of a relaxation mechanism in which lattice vibrations are coupled to the nuclear electric quadrupole moments. Usually, the effect of paramagnetic ions dominates the spin–phonon interaction for the relaxation time T_1 at very low temperature. However, the paramagnetic impurity effect on the spin–lattice relaxation process of Ga nuclei in β-Ga_2O_3:Cr^{3+} crystal was found to be very weak in the experimental temperature range.

References

[1] H.H. Tippins, Optical absorption and photoconductivity in the band edge of β-Ga_2O_3, Phys. Rev. 140 (1965) A316–A319.
[2] N. Ueda, H. Hosono, R. Waseda, H. Kawazoe, Anisotropy of electrical and optical properties in β-Ga_2O_3 single crystals, Appl. Phys. Lett. 71 (1997) 933–935.
[3] S. Geller, Crystal structure of β-Ga_2O_3, J. Chem. Phys. 33 (1960) 676–684.
[4] T. Xiao, A.H. Kitai, G. Liu, A. Nokua, J. Barbier, Thin film electroluminescence in highly anisotropic oxide materials, Appl. Phys. Lett. 72 (1998) 3356–3358.
[5] T. Minami, T. Shirai, T. Nakatani, T. Miyata, Electroluminescent devices with Ga_2O_3: Mn thin-film emitting layer prepared by sol-gel processes, Jpn. J. Appl. Phys. 39 (2000) L524–L526.
[6] Z. Hajnal, J. Miro, G. Kiss, F. Reti, P. Deak, R.C. Herndon, J.M. Kuperberg, Role of oxygen vacancy defect states in the n-type conduction of β-Ga_2O_3, J. Appl. Phys. 86 (1999) 3792–3796.
[7] R. Roy, V.G. Hill, E.F. Osborn, Polymorphism of Ga_2O_3 and the system Ga_2O_3-H_2O, J. Am. Chem. Soc. 74 (1952) 719–722.
[8] H. Makino, S. Nakamura, K. Matsumi, Lattice parameter variations in Czochralski grown gadolinium gallium garnet single crystals, Jpn. J. Appl. Phys. 15 (3) (1976) 415–419.
[9] J. Ahman, G. Svensson, J. Albertsson, A reinvestigation of β-gallium oxide, Acta Crystallogr. C52 (1996) 1336–1338.
[10] SGTE Database SPS96TO2 (pure substances), 1996.
[11] M. Ueltzen, The verneuil flame fusion process: substances, J. Cryst. Growth 132 (1-2) (1993) 315–328.
[12] T. Vosegaard, I.P. Byriel, L. Binet, D. Massiot, H.J. Jakobsen, Crystal structure studies by single crystal NMR spectroscopy. ^{71}Ga and ^{69}Ga single crystal NMR of β-Ga_2O_3 twins, J. Am. Chem. Soc. 120 (1998) 8184–8188.
[13] W. Gunsser, K. Rohwer, Detremination of the correlation between the crystal field axis system and the crystallographic axes in chromium-doped β-Ga_2O_3 by EPR, Phys. Status Solidi B 116 (1983) 275–278.
[14] T.H. Yeom, I.G. Kim, S.H. Lee, S.H. Choh, Y.M. Yu, Electron paramagnetic resonance characterization of Cr^{3+} impurities in a β-Ga_2O_3 single crystal, J. Appl. Phys. 93 (2003) 3315–3319.
[15] M.J. Mombourquette, J.A. Weil, D.G. McGavin, Operating Instruction for Computer Program EPR-NMR Ver. 6.0, University of Saskatchewan, Canada, 1995.
[16] G. Burns, Polarizabilities and antishielding factors of 10 and 18 electron closed shell atoms, J. Chem. Phys. 31 (1959) 1253–1255.
[17] G.M. Wolten, A.B. Chase, Determination of the point group of β-Ga_2O_3 from morphology and physical properties, J. Solid Chem. 16 (1976) 377–383.
[18] T.H. Yeom, K.T. Han, S.H. Choh, K.S. Hong, ^{7}Li NMR relaxation in a $LiTaO_3$ single crystal, J. Korean Phys. Soc. 28 (1995) 113–115.
[19] R.L. Mieher, Quadrupolar nuclear relaxation in the III-V compounds, Phys. Rev. 125 (1962) 1537–1551.
[20] A. Abragam, The Principles of Nuclear Magnetism, Oxford University Press, Oxford, 1961 (Chapters I and IX).
[21] T.H. Yeom, K.S. Hong, I. Yu, H.W. Shin, S.H. Choh, Spin-lattice relaxations of ^{9}Be and ^{27}Al in single crystalline alexandrite, J. Appl. Phys. 82 (1997) 2472–2475.
[22] J. Van Kranendonk, Theory of quadrupolar nuclear spin-lattice relaxation, Physica 20 (1954) 781–800.
[23] J.J. van der Klink, D. Rytz, F. Borsa, U.T. Hochli, Collective effects in a random-site electric dipole system: $KTaO_3$: Li, Phys. Rev. B27 (1983) 89–101.
[24] R. Blinc, J. Dolinsek, B. Zalar, Low temperature properties of proton and deuteron glasses, Z. Phys. B104 (1997) 629–634.
[25] B. Cowan, Nuclear Magnetic Resonance and Relaxation, Cambridge University Press, Cambridge, 1997.
[26] J. Dolinsekk, D. Arcon, B. Zalar, R. Pirc, R. Blinc, R. Kind, Quantum effects in the dynamics of proton glasses, Phys. Rev. B 54 (1996) R6811–R6814.
[27] C.P. Poole, H.A. Farach, Relaxation in Magnetic Resonance, Academic Press, New York, 1971 (Chapter 10).